



Equilibrium and dynamical properties of few particle systems in single and coupled e-h-quantum dots

A.V. Filinov^{1,2}, V. Golubnychiy¹, P. Ludwig¹, M. Bonitz¹, and Yu.E. Lozovik²

¹ Fachbereich Physik, Universität Rostock, ² Institute of Spectroscopy, Russian Academy of Sciences, 142190 Troitsk

1 Introduction

- Mesoscopic electron systems in quantum dots are known to reveal interesting correlation effects, e.g. Wigner crystallization [2]
- **Extensions in present work:** 1. Single-electron control of melting/conductivity [1] confirmed by dynamic simulation. 2. Generalization to mesoscopic electron-hole *bilayers* (vertically coupled quantum dots): crystallization of excitons observed, energy spectrum is found.

2 Single-electron control of circular current in quantum dots

- Investigation of the response of mesoscopic 2D electron clusters to external angular excitation.
- Control of the angular current by addition/removal of a single electron \Rightarrow application to single-electron devices [1].
- Idea: use the striking difference of orientational melting temperatures of cluster with $N = 19, 20$, see Fig. 1, to switch between liquid-like (“conducting”) and crystal-like (“insulating”) behaviour [2].

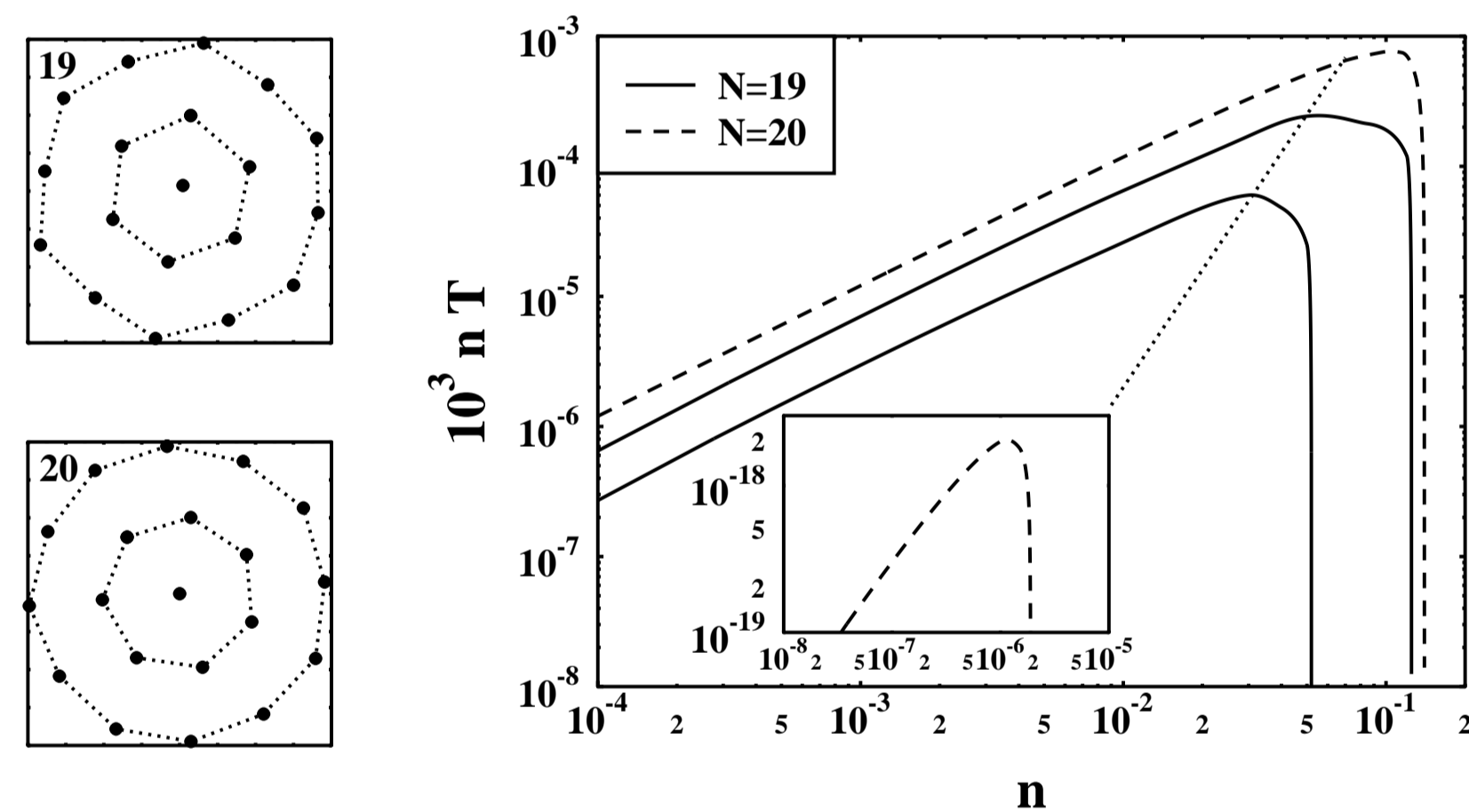


Fig. 1 Left: Ground state configuration of $N = 19$ and $N = 20$ clusters. Right: Phase diagram of the “crystal” phases for $N = 19, 20$. The outer (inner) lines are the radial (angular) melting phase boundaries. The classical melting takes place at specific values of the coupling parameters: $\Gamma_{20}^{RM} = 83$, $\Gamma_{19}^{RM} = 154$, $\Gamma_{19}^{OM} = 330$ and $\Gamma_{20}^{OM} = 3.4 \cdot 10^{11}$. $\Gamma = \left(\frac{e^2}{k_B T}\right) \left(\frac{e a}{k_B T}\right)$.

2.1 Model and simulation idea

Hamiltonian of a single quantum dot:

$$\hat{H} = -\sum_{i=1}^N \frac{\hbar^2 \nabla_i^2}{2m_i} + \sum_{i=1}^N \frac{m_j \omega_0^2 r_i^2}{2} + \sum_{i < j} \frac{e^2}{\epsilon |\mathbf{r}_i - \mathbf{r}_j|}$$

After reaching the ground state configuration (see above) the system is disturbed by: (1) *angular external force*, (2) friction. We calculate the response by solving:

$$m_e \ddot{v}_i(t) = \sum_{i,j} \vec{F}_{ij} + \vec{F}_i^{ext} - \gamma \dot{v}_i(t), \quad i = 1, \dots, N$$

- External force, $\vec{F}_i^{ext} = const$, acts only on the outer shell.
- To prevent rotation of the cluster as whole we pinned *one particle of the inner shell*, it allows to move only radially.
- One particle is *slowly* added/removed to the inner shell.

Result: I) Angular current (intershell rotation) flows in $N = 20$ cluster and stops after removal of 20-th particle.

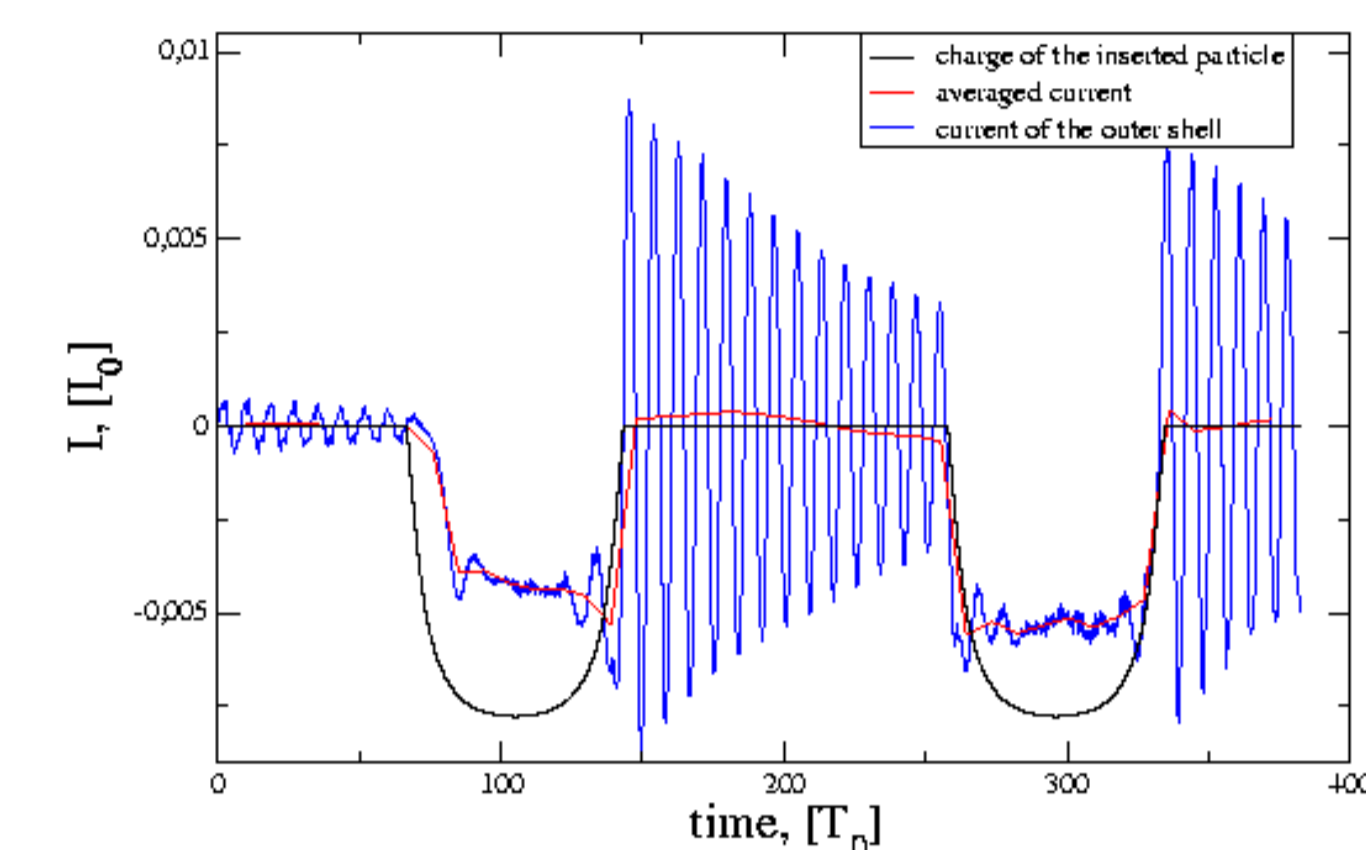


Fig. 2: Dependence of the outer shell current on time. Averaged current is also shown. Black line is the charge of the inserted particle. Time is in units of $T_0 = 2\pi/\omega_0$. Units of current is $I_0 = e\frac{v_0}{T_0}$, with unit of length $r_0 = \left(\frac{2e^2}{\epsilon m \omega_0^2}\right)^{1/3}$.

II) We demonstrate principal possibility of creation the device with open and close states. The inserted particle should be inserted about $30 T_0$, friction coefficient should be chosen to ensure steady constant current in open state.

3 Mesoscopic electron-hole bilayer systems

Hamiltonian of two vertically coupled electron-hole QD's:

$$\hat{H} = H_e + H_h - \sum_{i=1}^{N_e} \sum_{j=1}^{N_h} \frac{e_i e_j}{\epsilon \sqrt{|\mathbf{r}_i - \mathbf{r}_j|^2 + d^2}}$$

$$\hat{H}_{e(h)} = \sum_{i=1}^{N_{e(h)}} \left[-\frac{\hbar^2}{2m_i} \nabla^2 + V_{e(h)}(\mathbf{r}_i) + \sum_{i < j} \frac{e_i e_j}{\epsilon |\mathbf{r}_i - \mathbf{r}_j|} \right]$$

We consider symmetrical bilayers: $m_e = m_h = m$. Confinement potentials are equal: $V_e = V_h = \frac{1}{2} m \omega^2 r^2$.

The state of the system is governed by two competing effects:

- *Intra-layer* Coulomb repulsion of particles \rightarrow “crystallization” in each layer
- *Inter-layer* attraction between electrons and holes \rightarrow formation of inter-well excitons (or dipoles in the classical limit)

3.1 Classical mesoscopic bilayers

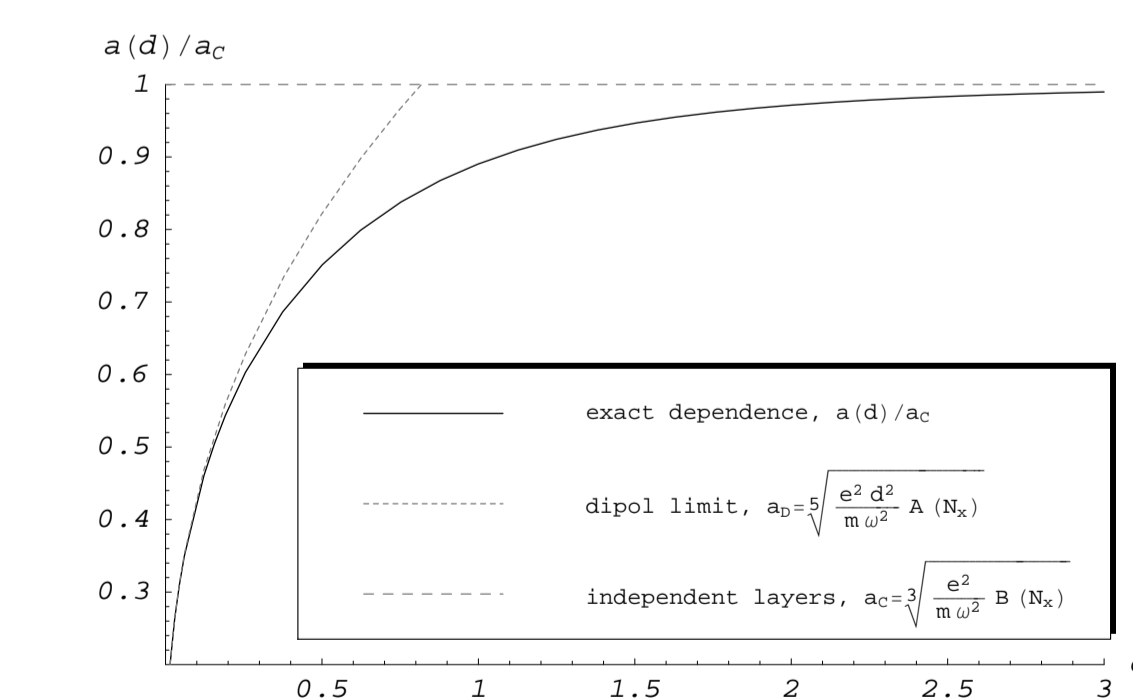


Fig. 4 Intra-layer particle distance, $a(d)$, in the ground state as a function of layer separation d (the unit of length is a_c). We have two limits: (I) $d \ll 1$, $a(d)$ is determined only by dipole-dipole interaction (mean interparticle distance a_D), (II) $d \gg 1$, intra-layer Coulomb interaction dominates (mean distance a_C). Note the different power laws of $a(d)$ in the two limits.

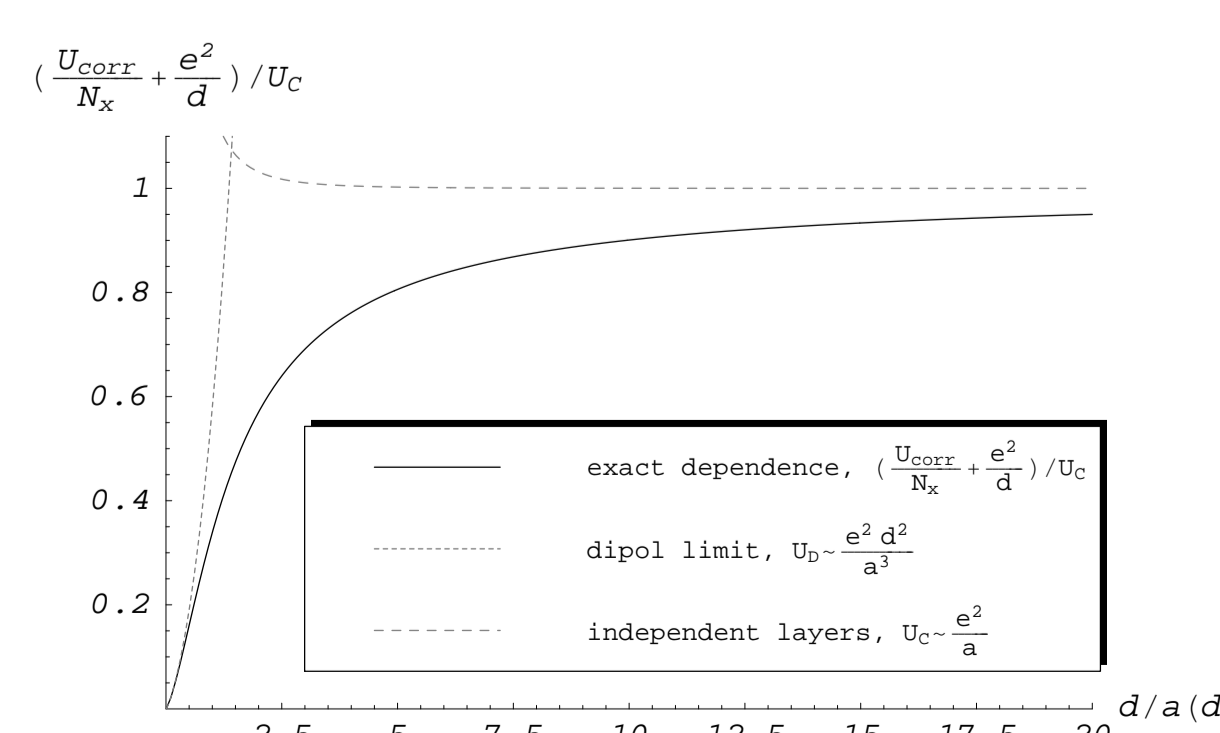


Fig. 5 Correlation energy (binding energy of excitons is excluded) for different distances between layers, d . Figure compares the exact correlation energy with the two limits: system of dipoles, U_D , and independent layers, U_C .

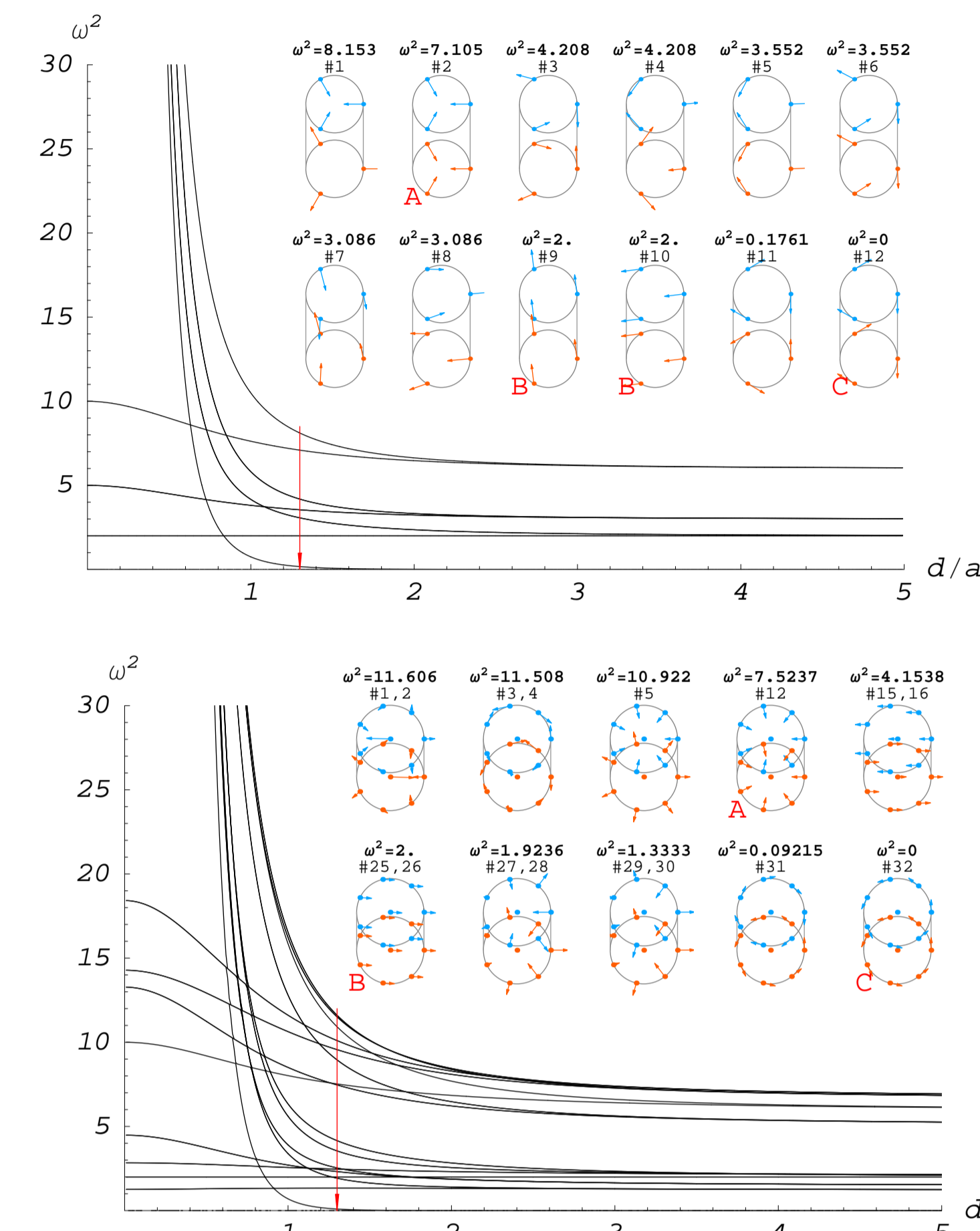


Fig. 6, 7 Excitation spectrum of normal modes for three and eight excitons as a function of distance d . The eigenfrequencies, ω , are in units of the trap frequency divided by $\sqrt{2}$. There are always $2N$ normal modes. Insets display the eigenvectors and eigenvalues for $d/a = 1.3$ (in descending order) computed from the Hesse-Matrix: $H_{ij} = \partial^2 H / \partial r_i \partial r_j$, $\vec{r} = \{x_1, y_1, \dots, x_N, y_N\}$ is a vector of all particle coordinates.

For all systems one always finds three trivial, universal modes:

- rotation of the whole system*, $\omega^2 = 0$,
- vibration of the center of mass*, $\omega^2 = 2$ (two-fold degenerate),
- breathing mode*, exact result for general interaction of the form $U \sim \frac{e^2}{a^{1+p}}$:

$$\omega_{br}^2 = 2m(3+p) = \begin{cases} 6, & p=0 \text{ Coulomb} \\ 10, & p=2 \text{ dipole} \\ 14, & p=4 \text{ quadrupole} \end{cases}$$

For excitons $\omega_{br}^2 = 20$ (dipole interaction, $m = m_e + m_h$).

Result: Analysis of mode spectrum reveals:

- $d > 1$: anti-phase rotation of shells in the electron and hole layers has the lowest energy [mode 11 (Fig. 6) and 31 (Fig. 7)] \Rightarrow with increasing temperature/density the two layers become decoupled and excitons are destroyed.
- $d < 1$: lowest excitation energies are related to pairwise coupled motion of electrons and holes \Rightarrow crystal melting proceeds via transition from exciton crystal to exciton liquid (excitons are preserved).

3.2 Quantum mesoscopic bilayers

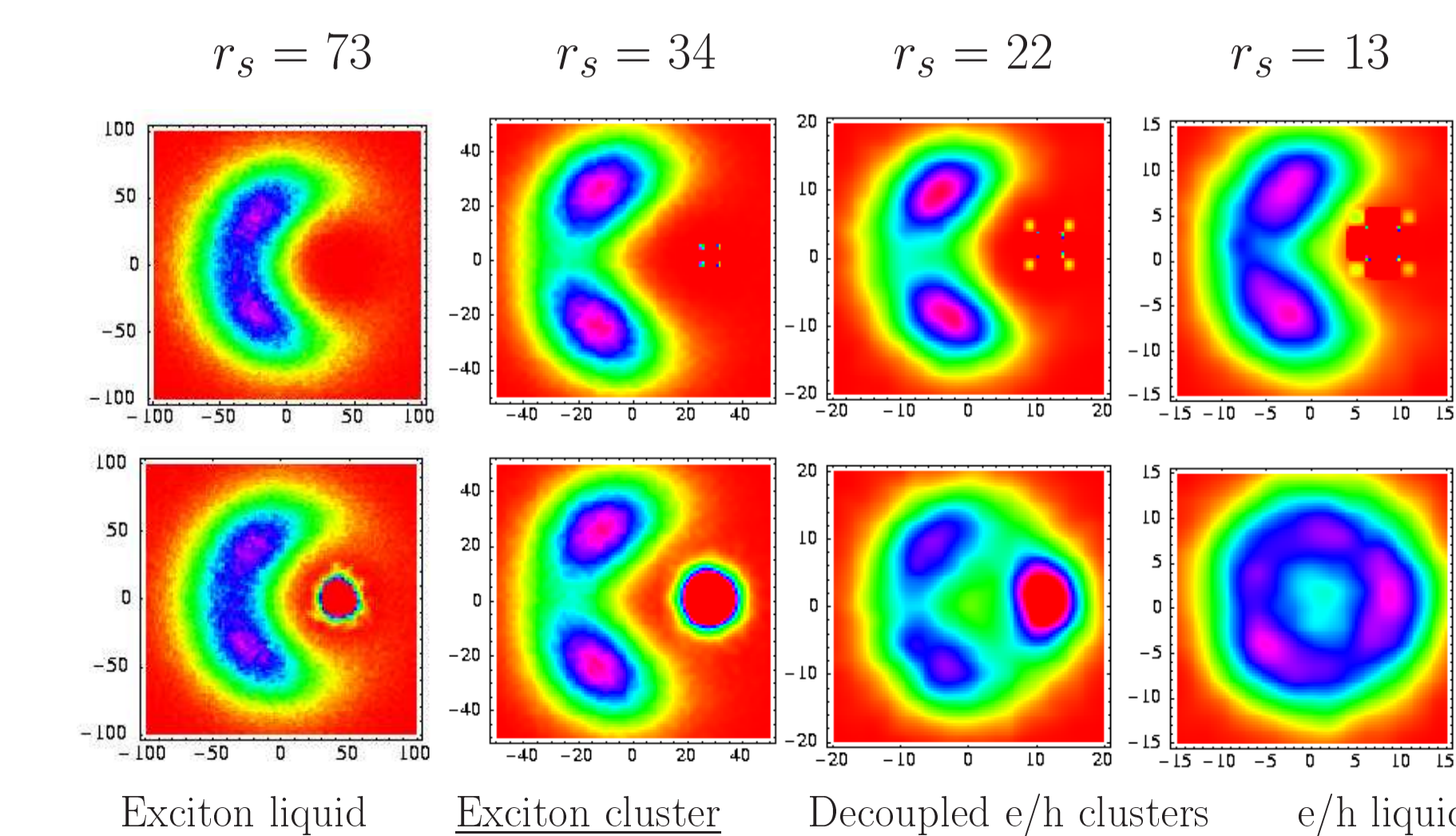


Fig. 5 Pair correlation function for 3 electrons and 3 holes (position of one electron is fixed), inter-layer distance $d = 10a_B$, temperature $T = 1/7 \times 10^{-3}$ Ha.

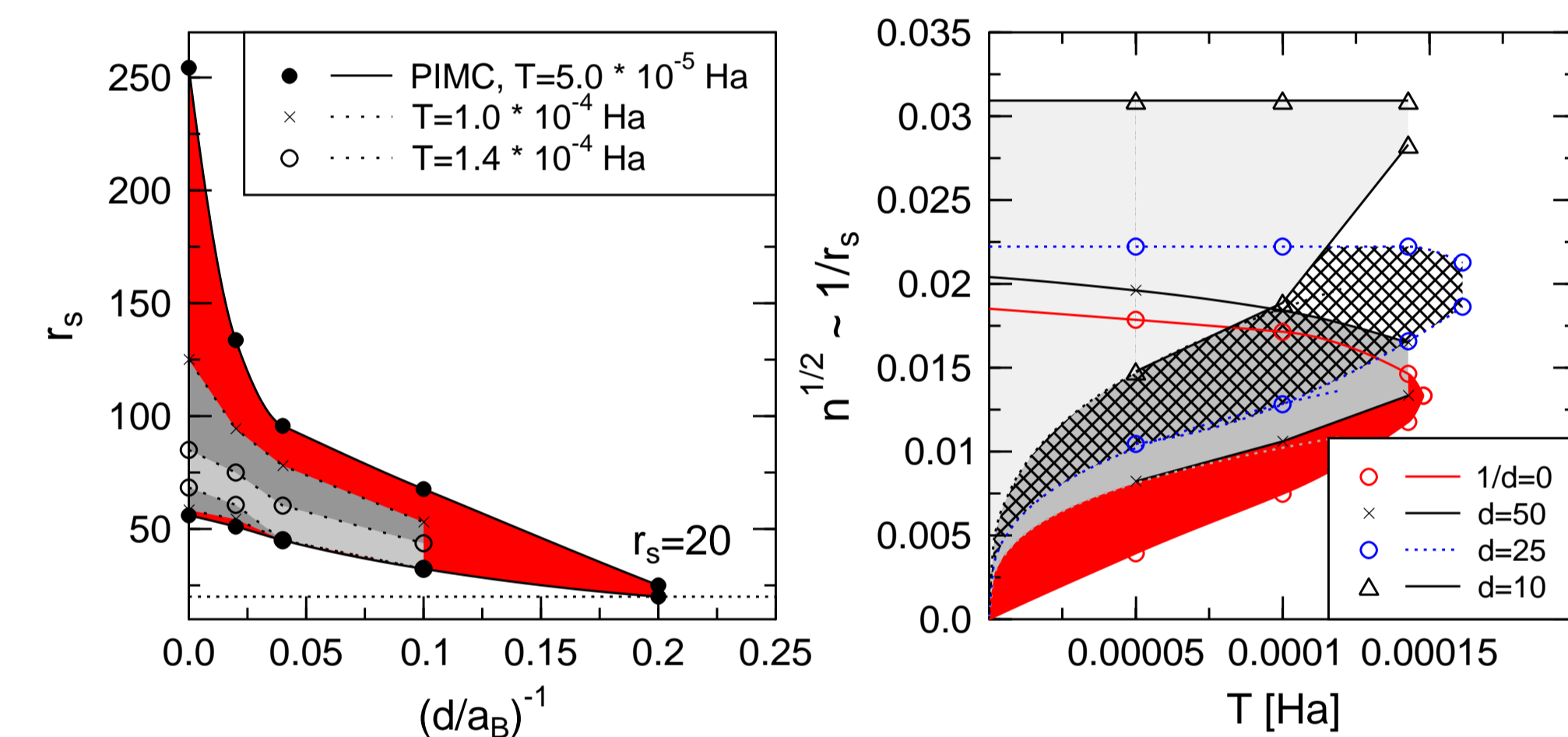
Results for temperature and density boundaries for the existence of e-h crystal: $T \lesssim 1/7 \times 10^{-3}$ Ha, $r_s \gtrsim 20$.

Examples:

- GaAs**-based structures: $T \lesssim 40$ mK and $\rho \lesssim 8 \times 10^8$ cm⁻²
- CdTe**-based structures: $T \lesssim 100$ mK and $\rho \lesssim 9 \times 10^9$ cm⁻²
- ZnSe**-based structures: $T \lesssim 400$ mK and $\rho \lesssim 3 \times 10^9$ cm⁻²

3.3 Phase diagram of e-h bilayers

- Exciton crystal* can exist only for inter-layer distances $d \gtrsim 5a_B$ and critical density parameter $r_s \gtrsim 20$.
- Interlayer attraction leads to stabilization of crystal phase: e.g., for exciton cluster, $N_e = N_h = 8$, coupling parameter r_s changes from $r_s \approx 56$ (for $d \rightarrow \infty$) to $r_s \approx 20$ (at $d = 5a_B$).
- Highest melting temperature is observed for intermediate $d \sim 25a_B$.



4 Summary and Outlook

- \Rightarrow Single-electron control of melting/conductivity is demonstrated.
- \Rightarrow Evidence for crystallization of excitons is found (not possible in single layers or for $d \lesssim 5a_B$).
- \Rightarrow Two crystal phases exist: exciton and decoupled e/h crystals.
- \Rightarrow Phase diagram (in T, n, d space) of mesoscopic e-h systems is presented.
- \Rightarrow (Classical) Excitation spectrum has been found and crystal melting scenario clarified.
- \Rightarrow Bose condensation of mesoscopic excitons expected at higher densities.

References

- [1] M. Bonitz, V. Golubnychiy, A.V. Filinov, Yu.E. Lozovik, *Microelectronic Engineering* **63**, 141 (2002)
- [2] A. Filinov, M. Bonitz and Yu.E. Lozovik, *Phys. Rev. Lett.* **86**, 3851 (2002)
- [3] An analysis of classical macroscopic e-h bilayers is performed in: P. Hartmann, Z. Donko, and G. Kalman, submitted to *Phys. Rev. Lett.*
- [4] Quantum macroscopic e-h bilayers has been investigated in: S. De Palo, F. Rapisarda, and G. Senatore, *Phys. Rev. Lett.* **88**, 206401 (2002)
- [5] G. Goldoni and F.M. Peeters, *Phys. Rev. B* **53**, 4591 (1996); I.V. Schweigert, V.A. Schweigert, and F.M. Peeters, *Phys. Rev. Lett.* **82**, 5293 (1999)